Regional Retinal Ganglion Cell Axon Loss in a Murine Glaucoma Model

Julie A. Schaub, Elizabeth C. Kimball, Matthew R. Steinhart, Cathy Nguyen, Mary E. Pease, Ericka N. Oglesby, Joan L. Jefferys, and Harry A. Quigley

Glaucoma Center of Excellence, Wilmer Ophthalmological Institute, Johns Hopkins University, Baltimore, Maryland, United States

Correspondence: Julie A. Schaub, Smith Building M002, Wilmer Eye Institute, Johns Hopkins University, 400 North Broadway, Baltimore, MD 21287, USA; jschaub6@jhmi.edu.

Submitted: February 28, 2017
Accepted: April 20, 2017

Citation: Schaub JA, Kimball EC, Steinhart MR, et al. Regional retinal ganglion cell axon loss in a murine glaucoma model. *Invest Ophthalmol Vis Sci*. 2017;58:2765–2773. DOI: 10.1167/iovs.17-21761

Purpose. To determine if retinal ganglion cell (RGC) axon loss in experimental mouse glaucoma is uniform in the optic nerve.

Methods. Experimental glaucoma was induced for 6 weeks with a microbead injection model in CD1 ($n = 78$) and C57BL/6 (B6, $n = 68$) mice. From epoxy-embedded sections of optic nerve 1 to 2 mm posterior to the globe, total nerve area and regional axon density (axons/1600 μm^2) were measured in superior, inferior, nasal, and temporal zones.

Results. Control eyes of CD1 mice have higher axon density and more total RGCs than control B6 mice eyes. There were no significant differences in control regional axon density in all mice or by strain (all $P > 0.2$, mixed model). Exposure to elevated IOP caused loss of RGC in both strains. In CD1 mice, axon density declined without significant loss of nerve area, while B6 mice had less density loss, but greater decrease in nerve area. Axon density loss in glaucoma eyes was not significantly greater in any region in either mouse strain (both $P > 0.2$, mixed model). In moderately damaged CD1 glaucoma eyes, and CD1 eyes with the greatest IOP elevation exposure, density loss differed by region ($P = 0.05$, $P = 0.03$, mixed model) with the greatest loss in the temporal and superior regions, while in severely injured B6 nerves superior loss was greater than inferior loss ($P = 0.01$, mixed model, Bonferroni corrected).

Conclusions. There was selectively greater loss of superior and temporal optic nerve axons of RGCs in mouse glaucoma at certain stages of damage. Differences in nerve area change suggest non-RGC responses differ between mouse strains.

Keywords: glaucoma, axon loss, regional, optic nerve head, mouse, retinal ganglion cell

The development and severity of injury to retinal ganglion cells (RGCs) in glaucoma are associated with exposure to aspects of intraocular pressure (IOP), including mean,[1] fluctuation,[2] and peak IOP.[3] IOP deforms the optic nerve head (ONH) through the translaminar pressure gradient between the intraocular and the orbital optic nerve tissues and by tensile stresses generated by the peripapillary sclera (PPS).[4] The resulting ONH deformation depends on the mechanical properties of the PPS and the ONH tissues that support RGC axons as they leave the eye. In eyes with glaucoma, ONH deformation disrupts anterograde and retrograde RGC axonal transport, leading to axon degeneration and RGC somal death by apoptosis.[5,6] Variations in PPS and ONH mechanical properties are likely to contribute to variations in susceptibility to glaucoma damage.

Mechanical interactions between the PPS and the ONH are important determinants of IOP-induced effects on RGC axons.[7] A better understanding of the biomechanical interplay of the ONH and PPS may improve predictions of the development and progression of glaucomatous axonal damage, leading to new therapeutic approaches.[8] The sclera has been studied by in vitro deformation mapping in human,[9] monkey,[10] and mouse,[11,12] exhibiting less strain in older eyes, in diagnosed human glaucoma, and in experimental glaucoma. In glaucoma human eyes, scleral strain differed by region. In human and monkey eyes, RGC axon loss is greatest in the upper and lower poles of the ONH, where the relative density of connective tissue is lower.[13–15] This leads to areas of preferential visual field loss in glaucoma in the mid-peripheral visual field, which is subserved by axons passing through these more susceptible zones. Regions with lower connective tissue volume fraction are more compliant and thus incur larger IOP-produced strain.[16]

The mouse ONH contains no connective tissue, but has astrocytes exhibiting a similar physical configuration to the beams of the human lamina cribrosa,[17] with processes stretching across the ONH to permit passage of RGC axon bundles between them. The astrocytes are load-bearing, as shown in strain measurements in an explant model.[18] Mouse and rat eyes that are subjected to experimental increases in IOP have RGC, glial, and associated tissue alterations that are phenotypically similar to human glaucoma.[19,20] As in human glaucoma eyes, RGC axons in murine glaucoma have axonal transport obstruction at the ONH.[21] The pressure-strain behavior of the sclera demonstrates a stiffer and less anisotropic response after chronic IOP elevation. The normal mouse PPS has circumferential collagen and elastin fibers,[22] whose arrangement is altered by experimental glaucoma, as in human glaucoma.[23]

Selective loss of superior and inferior RGCs at the human ONH in glaucoma relates to the regional structure and mechanical behavior of the ONH. In rats, it has been suggested

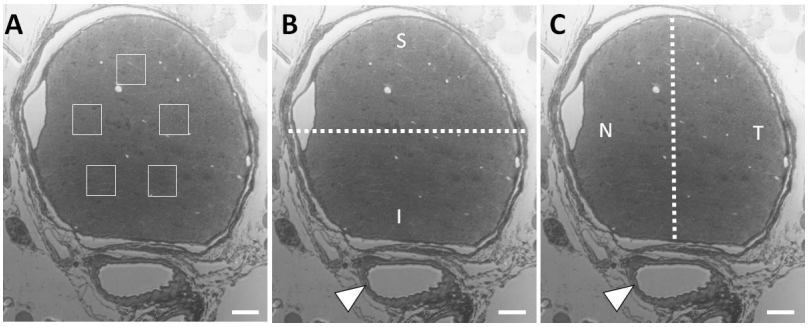

FIGURE 1. Diagram of selected zones for measuring axon density by regions. (**A**) Five 40 × 40-μm images (*white squares*) were acquired from the optic nerve, with the inferior pole identified by the presence of the inferior arteriole (**B**, *white arrowhead*). At least two windows per region were then categorized into B: superior (S) versus inferior (I) region or C: nasal (N) versus temporal (T) regions. *Scale bar*: 30 μm.

that there is greater RGC loss in the superior retina and optic nerve in experimental glaucoma.[24–26] We have previously examined the mouse ONH in an ex vivo explant model, determining that strain in control mouse astrocytic lamina cribrosa is significantly greater in the nasal–temporal direction than in the inferior–superior or anterior–posterior directions.[20] Furthermore, the PPS opening for the ONH in control eyes became wider in the nasal–temporal direction and narrower in the superior–inferior direction with inflation to 30 mm Hg. Given this asymmetric ONH strain, we examined whether there are regional differences in RGC axon loss within the optic nerve in mice after 6 weeks of experimental IOP elevation[27] to determine if RGC loss was regionally greater in any meridian, and if it corresponded to regional differences in ONH strain.

METHODS

Animals

The experiments used a total of 78 Crl:CD1(ICR) (CD1) mice and 68 C57BL/6J (B6) mice. The number of mice included in individual analyses depended upon whether all data were acquired; for example, some animals did not have complete IOP data or lacked fellow, control nerve data. The CD1 albino mice were 4 months old and acquired from Charles River, Inc. (Wilmington, MA, USA). The B6 pigmented mice were 4 to 7 months old and were obtained from The Jackson Laboratory (Bar Harbor, ME, USA). All animals and experiments were conducted in accordance with guidelines set forth by the ARVO Statement for the Use of Animals in Ophthalmic and Vision Research, using protocols approved and monitored by the Johns Hopkins University School of Medicine Animal Care and Use Committee (Baltimore, MD, USA).

Chronic IOP Elevation Model

Mice were anesthetized with a mixture of ketamine (Fort Dodge Animal Health, Fort Dodge, IA, USA), xylazine (VedCo, Inc., Saint Joseph, MO, USA), and acepromazine (50, 10, and 2 mg/kg, respectively; Phoenix Pharmaceuticals, Burlingame, CA, USA). The anterior chamber of one eye per mouse was injected with Polybead Microspheres (Polysciences, Inc., Warrington, PA, USA), consisting of 2 μL of 6-μm-diameter beads, then 2 μL of 1-μm-diameter beads, followed by 1 μL viscoelastic compound (10 mg/mL sodium hyaluronate, Healon; Advanced Medical Optics, Inc., Santa Ana, CA, USA) through a 50-μm-diameter tip glass cannula, connected to a Hamilton syringe (Hamilton, Inc., Reno, NV, USA).[27] IOP was measured with the Tonolab tonometer (TioLat, Inc., Helsinki, Finland) under anesthesia by inhalation of isoflurane using the RC2–Rodent Circuit Controller (VetEquip, Inc., Pleasanton, CA, USA) during the 6 weeks after injection (five measurements in CD1 and up to seven measurements in the B6).

RGC Axon Loss

Six weeks after microbead injection and IOP elevation, mice were killed by exsanguination and perfusion fixed with aldehydes. The optic nerves from chronic IOP elevation and control eyes were postfixed in 1% osmium tetroxide, epoxy-embedded, and sectioned at 1 μm. Digital images of optic nerve cross-sections were taken at low power to measure the total optic nerve area in square millimeter. Then, 40 × 40-μm windows (×100 magnification, Cool Snap camera, Metamorph Image Analysis software; Molecular Devices, Downington, PA, USA) were acquired from five locations in a pentagonal pattern, comprising a 9% sample of the total nerve area (Fig. 1). A masked observer edited nonaxonal elements from each image, and the program calculated axon density (axons/1600 μm^2). For 126 CD1 and 106 B6 nerves (including both glaucoma and control eyes), the inferior region was identified by the presence of the inferior arterioles. For each nerve, the data from the five density windows were assigned to the superior, inferior, nasal, and temporal regions (Fig. 1). Overall nerve axon counts were determined by multiplying mean axon density by nerve area. Since the size and shape of the nerve changed, particularly in B6 mice, with glaucoma injury, it was not considered appropriate to attempt local axon counts by multiplying regional axon density by regional area.

Statistical Methods

Since our analyses included multiple regions of the same nerve, there was a potential for covariance. We therefore constructed mixed models that took into account correlations among repeated measurements of axon density from a single nerve or mouse. After examination of sample correlations and Akaike's Information Criterion for several plausible correlation structures, repeated measurements from the four regions were assumed to have the spatial correlation structure suggested by Matérn.[28] Measurements from the two eyes were assumed to have an exchangeable correlation structure. For all models, least squares means and 95% confidence limits were used to estimate mean axon density by region, strain, and/or eye. The Bonferroni method was used to adjust pairwise significance levels for multiple comparisons. Analysis of the difference in axon density between the glaucoma eye and the fellow eye included only the 48 CD1 mice and the 38 B6 mice with data available on both eyes. Mixed models with the spatial correlation structure described above were used to estimate

Table 1. Effect of Region and Strain on Axon Density in Control Eyes

	Regression Parameter		Axon Density	Adjusted Pairwise	
Region/Strain	Estimate (95% CI)	*P* Value	Least Squares Mean (95% CI)	Comparing Regions*	*P* Value
Region, 118 eyes	−11.9 (−27.5, 3.8)	0.34	1026 (981, 1071)		
Superior (S)	−2.8 (−18.4, 12.9)		1035 (990, 1080)	S, I	0.80
Inferior (I)	−7.8 (−29.0, 13.3)		1030 (985, 1075)	N, T	0.94
Nasal (N)	0 (reference)		1038 (993, 1082)		
Temporal (T)					
Strain					
CD1, 65 eyes	385.9 (333.6, 438.2)	<0.0001	1205 (1170, 1240)		
B6, 53 eyes	0 (reference)		819 (781, 858)		

See Methods for statistical model details. CI, confidence interval.
* Bonferroni adjustment for multiple comparisons.

mean difference in axon density by region and/or strain. Student's *t*-test was used to compare the two strains of mice on continuous variables roughly normally distributed in each strain. Statistical analyses were performed by using SAS 9.2 (SAS Institute, Cary, NC, USA).

Results

Control Regional Axon Density and Axon Count

Axon density is presented as the number of axons within image windows that were each 40 × 40 μm (hence, density = axons/1600 μm^2). In 118 control nerves of both mouse strains combined, the least squares means of regional axon density were just over 1000 axons/1600 μm^2, with no significant difference in mean density among the four regions ($P = 0.34$, mixed model; Table 1). In a separate model, the control CD1 mice had a higher axon density than control B6 mice ($P < 0.0001$, mixed model; Table 1). There were no significant differences in axon density among the four regions of the nerve in either CD1 or B6 mice ($P = 0.21$, $P = 0.62$, respectively, mixed model; Table 2). Nor was the effect of region on fiber density significantly different by strain ($P = 0.40$, mixed model; Table 2). To calculate total nerve axon counts, the nerve area was multiplied by the average axon density. Control CD1 mice had a higher total axon count than B6 controls (57,532 vs. 47,659; Table 3), as we have published in several past reports.

Density and Axon Counts in Glaucoma Eyes

In glaucoma nerves, there was a significant loss in total axon number for both strains (both $P < 0.0001$, mixed model; Table 3) produced by multiplying the mean axon density by the total nerve area. CD1 mice had a significantly higher mean percentage axon loss than B6 mice, 36% vs. 23%, respectively ($P = 0.005$, mixed model; Table 3). The axon density loss was greater in CD1 than in B6 mice ($P < 0.0001$ for strain difference, mixed model; Table 3), while the optic nerve area decreased twice as much in B6 as in CD1 ($P = 0.02$ for strain difference, mixed model; Table 3). The area loss in CD1 was not significant ($P = 0.23$, mixed model; Table 3). Thus, the percentage decreases in total axon number and in axon density in CD1 mice were similar with nearly unchanged nerve area. For B6 mice, the percentage decrease in axon number was 23%, but axon density declined only 14%, since the nerve area decreased appreciably (Table 3).

The data for each mouse strain were categorized into low, medium, and high percentage axon number loss, compared to pooled control eyes for that strain, determining that the axon density fell significantly as percentage axon loss increased ($P < 0.0001$ for both strains, mixed model; Fig. 2, Table 4).

In CD1 mice, the decrease in regional axon density in glaucoma nerves was highly significant in all four quadrants (all

Table 2. Control and Glaucoma Regional Axon Density by Strain

		Least Squares Mean (95% CI)	
Mouse Strain	Region	Control	Glaucoma
CD1, 65 eyes	Superior (S)	1197 (1160, 1235)	787 (707, 867)
	Inferior (I)	1210 (1173, 1248)	798 (718, 878)
	Nasal (N)	1195 (1157, 1233)	796 (716, 876)
	Temporal (T)	1219 (1181, 1257)	792 (713, 872)
	P value	0.21	0.92
B6, 53 eyes	Superior (S)	816 (774, 857)	691 (605, 777)
	Inferior (I)	820 (778, 862)	716 (631, 802)
	Nasal (N)	827 (786, 869)	694 (609, 780)
	Temporal (T)	815 (774, 857)	723 (637, 808)
	P value	0.62	0.29
P value for effect of strain on regional variation		0.40	0.68

See Methods for statistical methods. *P* values are given for difference in regional densities for each group and strain. CI, confidence interval.

Table 3. Effect of Glaucoma on Axon Number, Axon Density, and Nerve Area by Strain

Variable	Strain	Eye	Least Squares Mean (95% CI)	% Decrease	*P* Value Glaucoma*	*P* Value Strains†
Total axon number	CD1	Glaucoma/control	36,823 (33,404–40,242)/57,532 (54,217–60,847)	36	<0.0001	0.005
	B6	Glaucoma/control	36,547 (32,878–40,215)/47,659 (43,991–51,328)	23	<0.0001	
Overall axon density, axons/1600 μm²	CD1	Glaucoma/control	793 (733–854)/1205 (1,146–1,263)	34	<0.0001	<0.0001
	B6	Glaucoma/control	706 (641–771)/819 (754–884)	14	0.02	
Optic nerve area, mm²	CD1	Glaucoma/control	0.074 (0.070–0.077)/0.076 (0.073–0.079)	3	0.23	0.02
	B6	Glaucoma/control	0.084 (0.080–0.087)/0.093 (0.089–0.096)	10	<0.0001	

Number of mice per group: CD1 = 78, B6 = 68. Least squares means are from a mixed model.
* Mixed model comparison of control to glaucoma.
† Mixed model comparison of the effect of glaucoma in CD1 to B6; see Methods for statistical model details. CI, confidence interval.

$P < 0.0001$, mixed model). Density was also significantly lower in each region in B6 mice, though to a lesser degree than in CD1 (P value varied from 0.01 to 0.05, mixed model). Exposure to elevated IOP in the glaucoma model did not produce any significant differences among the regions in axon density of either CD1 or B6 mice ($P = 0.92$, $P = 0.29$, respectively; Table 5). The effect of region on fiber density was not significantly different by strain ($P = 0.68$, mixed model; Table 5).

Since we found no difference in density with glaucoma among the four regions in either mouse strain for all nerves, we next considered the hypothesis that regional density differences might only be detected at certain stages of injury or with particular IOP exposure levels. Thus, we constructed models that divided glaucoma nerves into low, medium, and high tertiles of percentage axon loss for their whole nerve, and then reexamined for the presence of regional density differences. In the high axon loss group, the density of the regions significantly differed ($P = 0.04$, mixed model) with the superior region having the lowest density (Table 6).

With CD1 mice divided into three axon loss severity groups, the medium group showed a significant difference by region ($P = 0.05$, mixed model), with the temporal and superior regions having the greater density losses (Fig. 3; Table 7). In the high axon loss group in CD1, the nasal region had the lowest density (Fig. 3).

With B6 glaucoma mice divided into three axon loss categories, a significantly greater density loss was seen in the superior region of the high axon loss group than in the inferior region ($P = 0.01$, mixed model, Bonferroni corrected; Table 8).

Effect of Intraocular Pressure

The glaucoma model caused significant mean increases in IOP in each mouse strain (mean peak IOP for CD1: 31.7 ± 9.1 mm Hg and for B6: 32.7 ± 12.5 mm Hg, compared to a control mean of 16.7 ± 2.1 mm Hg and 16.1 ± 2.5 mm Hg, respectively; both $P < 0.0001$, t-test). There was no difference in the degree of IOP increase between the two strains ($P > 0.05$, t-test). Peak, mean, and positive integral IOP levels were significantly higher with glaucoma treatment for CD1 and B6 mice (all $P < 0.0001$, t-test). CD1 mice were divided into three groups, as based on having had low, medium, or high positive integral IOP exposure. There were significant regional differences in axon density loss in both the low and the high positive integral IOP groups (both $P = 0.03$, mixed model; Fig. 4). In the high positive integral IOP group, the superior and temporal regions decreased more in axon density than inferior

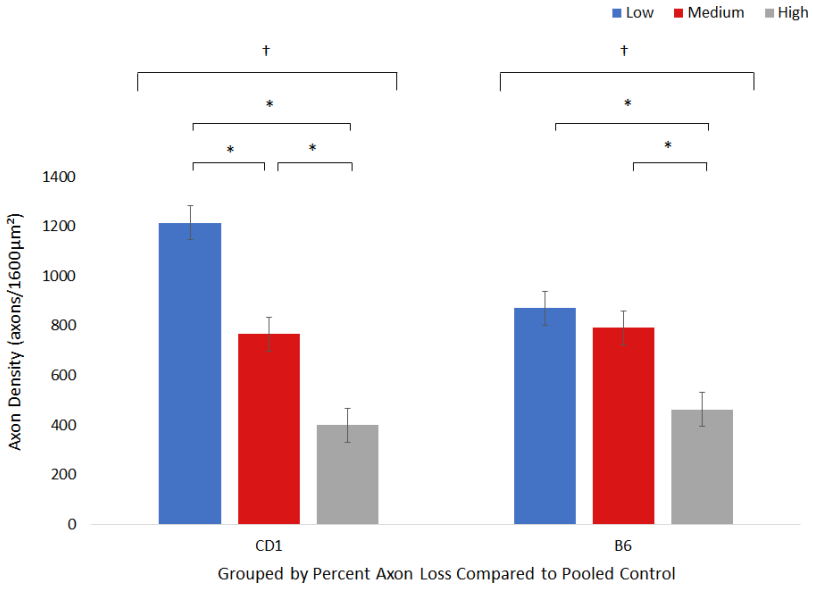

Figure 2. Axon density in 61 CD1 and 53 B6 mouse eyes divided into groups with low, medium, and high overall percentage RGC axon loss. *Groups that significantly differed in pairwise comparisons (all $P < 0.0003$, mixed model, Bonferroni corrected) (see Table 4 for data). †The percentage axon loss groups significantly differed by axon density in least squares means in both strains (both $P < 0.0001$, mixed model). *Error bars* denote 95% confidence interval.

Table 4. Axon Density in Glaucoma, by Severity of Axon Loss

Mouse Strain	% Axon Loss	Regression Parameter: Estimate (95% CI)	Regression Parameter: *P* Value	Axon Density: Least Squares Mean (95% CI)	Adjusted Pairwise: Comparing Categories*	Adjusted Pairwise: *P* Value
CD1, 61 eyes	55–97 (H)	−816 (−915, −717)	<0.0001	399 (330, 469)	H, M	<0.0003
	17.6–54 (M)	−449 (−547, −352)		766 (698, 834)	H, L	<0.0003
	Up to 17% (L)	0 (reference)		1215 (1146, 1285)	M, L	<0.0003
B6, 53 eyes	35–82 (H)	−408 (−500, −316)	<0.0001	462 (397, 527)	H, M	<0.0003
	6–34 (M)	−79 (−173, 14)		791 (724, 858)	H, L	<0.0003
	Up to 5.8% (L)	0 (reference)		870 (805, 935)	M, L	0.29

See Methods for statistical model details. CI, confidence interval; H, high; L, low; M, medium.
* Bonferroni adjustment for multiple comparisons.

and nasal regions. In the lowest positive integral IOP group, regional axon density decreased most nasally and inferiorly. There were no significant regional density differences with mice grouped into tertiles of peak IOP level in CD1 mice ($P = 0.16$, mixed model). In B6 mice, there were no significant differences in regional axon density between tertiles divided by positive integral or peak IOP parameters ($P = 0.33$, $P = 0.63$, respectively, mixed model). See Supplementary Material for tables of data points for each eye.

Discussion

Our data for all glaucoma nerves did not show any regional difference in loss of axon density, which is similar to data from a previous study in 559 DBA/2J spontaneous glaucoma mice, in which there is no regionally greater RGC loss in either retina or optic nerve.[29] However, it is important to consider that there is substantial variation in the degree of RGC loss in glaucoma models and strains. In eyes with mild loss, only small regional differences would be present, if any actually occurred. In eyes with severe loss, generalized damage might preclude detection of locally greater loss in a more susceptible region. Thus, we categorized our data by degree of axon loss and found that there was greater density loss in the superior and temporal nerve in moderately damaged CD1 nerves and in CD1 eyes with the greatest IOP exposure. The superior nerve region was also most affected in the most damaged B6 mice. Previous reports in rat experimental glaucoma[24–26] have found selectively greater superior RGC axon and cell body loss, as first suggested by Morrison et al.[30] One previous study of eight mouse eyes with laser-induced IOP elevation has found greater loss of axons in the inferior optic nerve,[31] while another modest study of genetically modified mice with elevated IOP has suggested greater loss in the peripheral retina compared to centrally.[32] The rat and mouse ONH structure differs in some details, yet it seems that the more susceptible region may be similar in the two rodent species.

Several studies of mouse and rat experimental glaucoma have identified sectorial (wedge-shaped) loss of RGCs emanating from the ONH. These reports have not found or have not commented on greater sectorial loss in one region of the retina.[29,33–37] The RGC loss in rat experimental glaucoma is also sectorial,[38] which is strong evidence that bundles of axons that are grouped together at the ONH are locally injured at that site.

Initial resistance to the use of rodent glaucoma models was overcome when it was recognized that mouse and rat eyes exhibit fundamental features of glaucoma when subjected to sustained IOP elevation. These include (1) injury to RGC axons at the ONH when IOP is chronically increased; (2) death of RGC bodies and their axons in the retina in a sectorial pattern, indicating injury in local zones of the ONH; and (3) selective loss of RGCs with sparing of other retinal neurons. While the mouse astrocytic lamina cribrosa has a similar general configuration to the connective tissue structure of the human lamina, there is no measurable regional difference in structure that we have found in quantitative volume fraction measurements.[18] With ex vivo inflation testing, there is greater strain in the nasal–temporal direction in normal mouse lamina.[18] The shape of the ONH canal as it passes through the mouse PPS is

Table 5. Regional Axon Density by Strain in Glaucoma Eyes

Strain	Region	Axon Density: Least Squares Mean (95% CI)	Axon Density: *P* Value Comparing Regions	Percentage Loss Compared to Pooled Control Eyes	Adjusted Pairwise: Comparing Regions*	Adjusted Pairwise: *P* Value
CD1, 61 eyes	Superior (S)	787 (707, 867)	0.92	34	S, I	1.00
	Inferior (I)	798 (718, 878)		34	N, T	1.00
	Nasal (N)	796 (716, 876)		33		
	Temporal (T)	792 (713, 872)		35		
				Overall = 34		
B6, 53 eyes	Superior (S)	691 (605, 777)	0.29	15	S, I	0.50
	Inferior (I)	716 (631, 802)		13	N, T	0.40
	Nasal (N)	694 (609, 780)		16		
	Temporal (T)	723 (637, 808)		11		
				Overall = 14		
P value for effect of strain on regional variation†			0.68			

* Bonferroni adjustment for multiple comparisons.
† Mixed model comparing the regional effect between strains; see Methods for statistical model details. CI, confidence interval.

Table 6. Regional Axon Density in All Glaucoma Eyes by Percentage Axon Loss

		Axon Density		Adjusted Pairwise	
% Axon Loss	Region	Least Squares Mean (95% CI)	*P* Value Comparing Regions	Comparing Regions*	*P* Value
High, 45–98, 38 eyes	Superior (S)	428 (360, 497)	0.04	S, I	0.03
	Inferior (I)	492 (423, 560)		N, T	0.29
	Nasal (N)	439 (370, 508)			
	Temporal (T)	476 (408, 545)			
Medium, 13–44.5, 38 eyes	Superior (S)	760 (691, 828)	0.68	S, I	1.00
	Inferior (I)	765 (696, 834)		N, T	0.96
	Nasal (N)	777 (709, 846)			
	Temporal (T)	759 (690, 828)			
Low, up to 12%, 38 eyes	Superior (S)	1039 (970, 1108)	0.66	S, I	1.00
	Inferior (I)	1023 (954, 1092)		N, T	1.00
	Nasal (N)	1030 (961, 1098)			
	Temporal (T)	1044 (976, 1113)			
P value for effect of % axon loss on regional variation†			0.20		

* Bonferroni adjustment for multiple comparisons.

† Mixed model comparing the regional effect among percentage axon loss groups; see Methods for statistical model details. CI, confidence interval.

horizontally oval, and this may contribute to this directional difference in measured strain. Furthermore, there is a group of large blood vessels just outside the ONH at its inferior border in mice that may provide an asymmetric effect on ONH strain. Consistent with these features, under inflation, the normal mouse ONH becomes significantly larger in the nasal–temporal direction and becomes narrower in the inferior–superior direction. Such asymmetric PPS deformation and laminar strain could be associated with greater axon loss in the dimension of narrowing, including the superior nerve. The cited mouse ONH strain measures have been carried out in Agouti mice, not in CD1 or B6 mice; we are presently engaged in regional RGC loss studies in Agouti mice to compare their behavior.

While there is regionally greater measured strain with inflation testing in the nasal–temporal direction in mouse ONH, this difference may not be the only explanation for differential RGC death. Injury and death of RGCs in rodent models occurs in weeks, while loss in human eyes is more chronic. The more rapid rate of loss in animal models may partially preclude regional selectivity. Selective damage in the human eye derives from regional structural and functional differences in lamina architecture that may not pertain to the mouse eye. It will be very interesting to determine what these interspecies differences may be, since their role could be illuminating for the mechanisms of glaucomatous optic neuropathy.

Our data demonstrated a difference in the detailed nature of optic nerve remodeling after experimental glaucoma damage in CD1 compared to B6 mice. Control B6 mice had fewer total RGC axons than CD1 mice, as well as a lower axon density. With chronic IOP exposure, CD1 eyes had a mean decrease in axon density of 34% and mean nerve axon count loss of 36%.

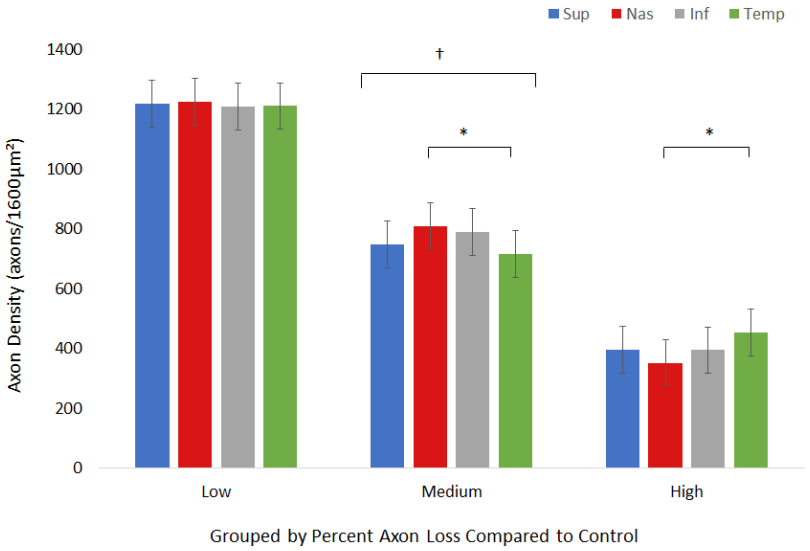

Figure 3. Axon density by region in 61 CD1 mouse eyes divided into groups with low, medium, and high overall percentage RGC axon loss. The axon density in least squares means by region differed among the three axon loss groups ($P = 0.02$, mixed model). *Indicates significant pairwise differences (medium group: $P = 0.03$, high group: $P = 0.02$, mixed model, Bonferroni corrected) (see Table 7 for data). †The effect of region on axon density in the medium group significantly varied ($P = 0.05$, mixed model). *Error bars* denote 95% confidence interval. Inf, inferior; Nas, nasal; Sup, superior; Temp, temporal regions.

Table 7. Regional Axon Density in CD1 Glaucoma Eyes by Percentage Axon Loss

		Axon Density		Adjusted Pairwise	
% Axon Loss	Region	Least Squares Mean (95% CI)	*P* Value Comparing Regions	Comparing Regions*	*P* Value
High, 55–98, 20 eyes	Superior (S)	396 (318, 473)	0.06	S, I	1.00
	Inferior (I)	395 (318, 473)		N, T	0.02
	Nasal (N)	353 (276, 431)			
	Temporal (T)	454 (376, 531)			
Medium, 17.5–54, 21 eyes	Superior (S)	748 (672, 824)	0.05	S, I	0.54
	Inferior (I)	789 (713, 865)		N, T	0.03
	Nasal (N)	810 (734, 886)			
	Temporal (T)	717 (641, 793)			
Low, up to 17.0%, 20 eyes	Superior (S)	1218 (1141, 1296)	0.96	S, I	1.00
	Inferior (I)	1209 (1131, 1287)		N, T	1.00
	Nasal (N)	1211 (1133, 1288)			
	Temporal (T)	1211 (1133, 1288)			
P value for effect of % axon loss on regional variation†			0.02		

* Bonferroni adjustment for multiple comparisons.

† Mixed model comparing the regional effect between percentage axon loss groups; see Methods for statistical model details. CI, confidence interval.

By contrast, the B6 nerves had a 14% reduction in axon density and 23% axon count loss. We performed axon diameter measurements, comparing control to glaucoma for both mouse strains. While the CD1 glaucoma mice had a 7% increase in mean axon diameter and the B6 had a 2% decrease in mean diameter (data not shown), these changes are far too small to account for the resultant nerve areas in the two groups of mice. Note that the myelinated nerve at the point of axon measurement here is outside the zone of local axon injury near to the eye. This suggests that the two mouse strains differ in how the nonaxonal, glial component of the optic nerve responds to loss of axons. CD1 mice undergo death of axons with minimal change in overall nerve area, indicating that there is a relative expansion of the glial compartment. B6 mice lose axons, but the nerve area shrinks proportionately, so that there is significantly smaller decline in axon density—pointing to a relatively greater loss of nonaxon tissue in the nerve. These differences in remodeling after glaucoma injury are worthy of further study, including within the ONH itself, which is the site of primary injury.

To quantify the number of axons by light microscopy, as in the present work, axons must be identified by the presence of their myelin sheath, which begins within 1 mm of the optic nerve in mice. Studies in the past by Minckler,[39] Hoyt,[40,41] and Radius[42] in cats and monkeys have looked at the distribution of axons in the optic nerve and tract, compared to their positions in the retina and optic nerve head. In the human anterior pathway, Hoyt and Luis[40] and Hoyt and Tudor[41] have demonstrated that while rearrangement of the chiasmal decussation begins in the orbital nerve, the axons of RGCs that are together in the nerve head do not randomly disperse, but rather keep sufficient topographic distribution. Radius and Anderson[42] have produced lesions in the retina and found that in the near optic nerve head region in monkeys, axons are still grouped together. The organization in mice may differ, but might be expected to have less need for redistribution, since

Table 8. Regional Axon Density in B6 Glaucoma Eyes by Percentage Axon Loss

		Axon Density		Adjusted Pairwise	
% Axon Loss	Region	Least Squares Mean (95% CI)	*P* Value Comparing Regions	Comparing Regions*	*P* Value
High, 35–82, 18 eyes	Superior (S)	423 (354, 493)	0.06	S, I	0.01
	Inferior (I)	503 (433, 572)		N, T	1.00
	Nasal (N)	467 (397, 536)			
	Temporal (T)	455 (386, 525)			
Medium, 6–34, 17 eyes	Superior (S)	791 (720, 863)	0.06	S, I	1.00
	Inferior (I)	781 (709, 852)		N, T	0.05
	Nasal (N)	761 (690, 833)			
	Temporal (T)	830 (758, 902)			
Low, up to 5.8%, 18 eyes	Superior (S)	864 (795, 934)	0.54	S, I	1.00
	Inferior (I)	869 (799, 938)		N, T	0.62
	Nasal (N)	859 (789, 928)			
	Temporal (T)	888 (819, 958)			
P value for effect of % axon loss on regional variation†			0.10		

* Bonferroni adjustment for multiple comparisons.

† Mixed model comparing the regional effect among percentage axon loss groups; see Methods for statistical model details. CI, confidence interval.

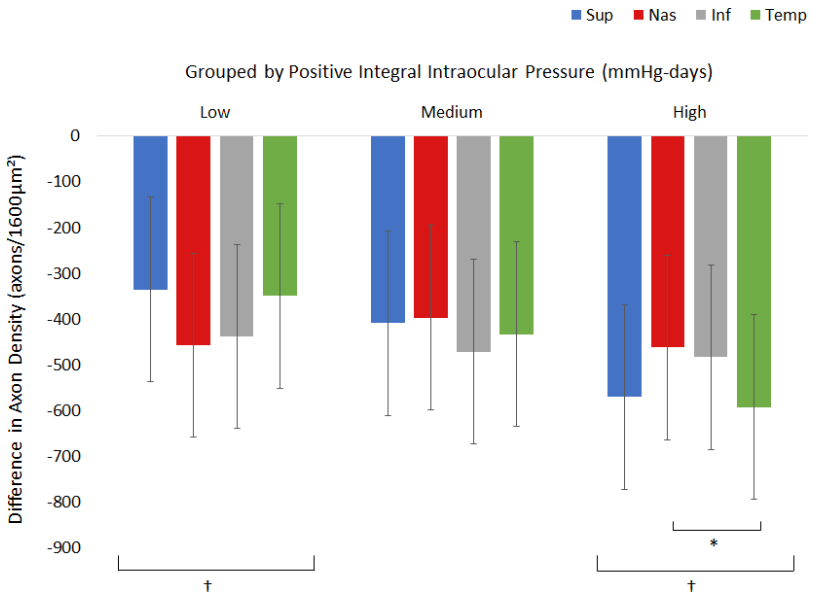

FIGURE 4. Regional axon density loss (difference in glaucoma from fellow eye) in 48 CD1 mice grouped into three categories by exposure to elevated IOP: low, medium, and high positive integral IOP (mm Hg–days). The axon density in least squares means by region differed among the three IOP groups ($P = 0.002$, mixed model). *The temporal region had significantly greater loss than nasal region in the high IOP exposure group in pairwise comparison ($P = 0.03$, mixed model, Bonferroni corrected). †The effect of region on axon density in the low and high groups significantly varied (both $P = 0.03$, mixed model). *Error bars* denote 95% confidence interval. Inf, inferior; Nas, nasal; Sup, superior; Temp, temporal regions.

most fibers simply cross at the chiasm, compared to primates in which they divide into ipsilateral and contralateral groups. We have studied mice with a subset of RGCs that is selectively fluorescent, permitting the tracking of individual axons in the zone studied in this study, 1 mm behind the sclera at the first segment of axons that are myelinated.[43] Axons follow generally straight courses without dramatic deviation from position in the first 3 mm behind the eye. Thus, the degree of rearrangement at the position studied here is highly relevant to their position at the site of injury, the optic nerve head.

We studied regional differences in axon loss in the optic nerve, but similar studies could be carried out in retinal whole mounts. The advantage of nerve data are that axons are easily detected, while in the retina it is necessary to label retinal ganglion cells either by backfilling with dye or with stains or antibodies. The latter are not always uniquely specific to RGCs and may not continue to identify RGCs when initial neuronal injury has occurred. The area occupied by the retina after globe enlargement in the glaucoma models has not been quantified; hence, we do not know if the retinal area changes, altering the calculation of retinal RGC density measurements by changing their denominator. As an example of how this issue could be relevant, optic nerve area did contract in B6 nerves. The decrease in overall nerve area, which might be regionally different, could give rise to relative repositioning of our chosen locations for axon density measurement when atrophy is severe. This caveat seems not to affect the CD1 nerve, which does not shrink in area with axon loss. Hence, we feel confident that the regional differences reported here are valid indicators of regional differences. We will report soon a large study in which both retinal whole mounts and optic nerve regional data from the same eyes will be compared to emphasize these points.

In summary, we found selectively greater loss of RGC axons, especially in the superior mouse optic nerve at some stages of experimental glaucoma. Previous investigations have found that RGCs die in wedge-shaped sectors whose axons converge to local areas of the ONH. Differences among mouse strains in the susceptibility and patterns of RGC loss in regions of the retina and optic nerve near the globe may provide information on mechanisms of glaucoma damage. When rodent glaucomatous optic neuropathy differs from the primate and human features, the differences may illuminate relevant anatomic or physiological factors that are identifiable precisely because of interspecies differences.

Acknowledgments

Supported in part by Public Health Service (PHS) Research Grants EY 02120 and EY 01765 (HAQ, and Wilmer Institute Core grant) and by unrestricted support from Saranne and Livingston Kosberg and from William T. Forrester. The funders had no role in study design, data collection and analysis, decision to publish, or preparation of the manuscript.

Disclosure: **J.A. Schaub**, None; **E.C. Kimball**, None; **M.R. Steinhart**, None; **C. Nguyen**, None; **M.E. Pease**, None; **E.N. Oglesby**, None; **J.L. Jefferys**, None; **H.A. Quigley**, None

References

1. Bengtsson B, Heijl A. Diurnal IOP fluctuation: not an independent risk factor for glaucomatous visual field loss in high-risk ocular hypertension. *Graefes Arch Clin Exp Ophthalmol*. 2005;243:513–518.
2. Nouri-Mahdavi K, Hoffman D, Coleman A. Predictive factors for glaucomatous visual field progression in the Advanced Glaucoma Intervention Study. *Ophthalmology*. 2004;111:1627–1635.
3. De Moraes CG, Juthani VJ, Liebmann JM. Risk factors for visual field progression in treated glaucoma. *Arch Ophthalmol*. 2011;129:562–568.
4. Burgoyne CF, Downs JC, Bellezza AJ, Suh JK, Hart RT. The optic nerve head as a biomechanical structure: a new paradigm for understanding the role of IOP-related stress and strain in the pathophysiology of glaucomatous optic nerve head damage. *Prog Retin Eye Res*. 2005;24:39–73.
5. Quigley HA, Nickells RW, Kerrigan LA, Pease ME, Thibault DJ, Zack DJ. Retinal ganglion cell death in experimental glaucoma

and after axotomy occurs by apoptosis. *Invest Ophthalmol Vis Sci*. 1995;36:774–786.

6. Kerrigan LA, Zack DJ, Quigley HA, Smith SD, Pease ME. TUNEL-positive ganglion cells in human primary open angle glaucoma. *Arch Ophthalmol*. 1997;115:1031–1035.
7. Sigal IA, Yang H, Roberts MD, Burgoyne CF, Downs JC. IOP-induced lamina cribrosa displacement and scleral canal expansion: an analysis of factor interactions using parameterized eye-specific models. *Invest Ophthalmol Vis Sci*. 2011;52:1896–1907.
8. Quigley HA, Pitha IF, Welsbie DS, et al. Losartan treatment protects retinal ganglion cells and alters scleral remodeling in experimental glaucoma. *PLoS One*. 2015;10:e0141137.
9. Coudrillier B, Pijanka JK, Jefferys JL, et al. Glaucoma-related changes in the mechanical properties and collagen microarchitecture of the human sclera. *PLoS One*. 2015;10:e0131396.
10. Girard MJA, Suh J-KF, Mottlang M, Burgoyne CF, Downs JC. Biomechanical changes in the sclera of monkey eyes exposed to chronic IOP elevations. *Invest Ophthamol Vis Sci*. 2011;52:5656–5669.
11. Myers KM, Cone FE, Quigley HA, Gelman SE, Pease ME, Nguyen TD. The in vitro inflation response of mouse sclera. *Exp Eye Res*. 2010;91:866–875.
12. Nguyen C, Cone FE, Nguyen TD, et al. Studies of scleral biomechanical behavior related to susceptibility for retinal ganglion cell loss in experimental mouse glaucoma. *Invest Ophthalmol Vis Sci*. 2013;54:1767–1780.
13. Quigley HA, Addicks EM. Regional differences in the structure of the lamina cribrosa and their relation to glaucomatous optic nerve damage. *Arch Ophthalmol*. 1981;99:137–143.
14. Dandona L, Quigley HA, Brown AE, Enger C. Quantitative regional structure of the normal human lamina cribrosa: a racial comparison. *Arch Ophthalmol*. 1990;108:393–398.
15. Quigley HA, Addicks EM, Green WR. Optic nerve damage in human glaucoma, III: quantitative correlation of nerve fiber loss and visual field defect in glaucoma, ischemic neuropathy, disc edema, and toxic neuropathy. *Arch Ophthalmol*. 1982;100:135–146.
16. Midgett DE, Pease ME, Quigley HA, Patel M, Franck C, Nguyen TD. The pressure-induced deformation response of the human lamina cribrosa: analysis of regional variations. *Acta Biomater*. 2017;53:123–139.
17. Sun D, Lye-Barthel M, Masland RH, Jakobs TC. The morphology and spatial arrangement of astrocytes in the optic nerve head of the mouse. *J Comp Neurol*. 2009;516:1–19.
18. Nguyen C, Midgett DE, Kimball FE, et al. Measuring deformation in the mouse optic nerve head and peripapillary sclera. *Invest Ophthalmol Vis Sci*. 2017;58:721–733.
19. Morrison JC, Cepurna WO, Guo Y, Johnson EC. Pathophysiology of human glaucomatous optic nerve damage: insights from rodent models of glaucoma. *Exp Eye Res*. 2011;93:156–164.
20. Fernandes KA, Harder JM, Williams PA, et al. Using genetic mouse models to gain insight into glaucoma: past results and future possibilities. *Exp Eye Res*. 2015;141:42–56.
21. Howell GR, Libby RT, Jakobs TC, et al. Axons of retinal ganglion cells are insulted in the optic nerve early in DBA/2J glaucoma. *J Cell Biol*. 2007;179:1523–1537.
22. Pijanka JK, Coudrillier B, Ziegler K, et al. Quantitative mapping of collagen fiber orientation in non-glaucoma and glaucoma posterior human sclerae. *Invest Ophthalmol Vis Sci*. 2012;53:5258–5270.
23. Pijanka JK, Cone-Kimball E, Pease ME, et al. Changes in scleral collagen organization associated with murine chronic experimental glaucoma. *Invest Ophthalmol Vis Sci*. 2014;55:6554–6564.
24. Johnson EC, Deppmeier LMH, Wentzien SKF, Hsu I, Morrison JC. Chronology of optic nerve head and retinal responses to elevated intraocular pressure. *Invest Ophthalmol Vis Sci*. 2000;41:431–442.
25. Kwong JMK, Vo N, Quan A, et al. The dark phase intraocular pressure elevation and retinal ganglion cell degeneration in a rat model of experimental glaucoma. *Exp Eye Res*. 2013;112:21–28.
26. WoldeMussie E, Ruiz G, Wijono M, Wheeler LA. Neuroprotection of retinal ganglion cells by brimonidine in rats with laser-induced chronic ocular hypertension. *Invest Ophthalmol Vis Sci*. 2001;41:2849–2855.
27. Cone FE, Steinhart MR, Oglesby EN, Kalesnykas G, Pease ME, Quigley HA. The effects of anesthesia, mouse strain, and age on intraocular pressure and an improved murine model of experimental glaucoma. *Exp Eye Res*. 2012;99:27–35.
28. Matérn B. *Spatial Variation, Lecture Notes in Statistics*. 2nd ed. New York City, NY: Springer-Verlag; 1986.
29. Schlamp CL, Li Y, Dietz JA, Janssen KT, Nickells RW. Progressive ganglion cell loss and optic nerve degeneration in DBA/2J mice is variable and asymmetric. *BMC Neurosci*. 2006;7:66.
30. Morrison JC, Moore CG, Deppmeier LM, Gold BG, Meshul CK, Johnson EC. A rat model of chronic pressure-induced optic nerve damage. *Exp Eye Res*. 1997;64:85–96.
31. Mabuchi F, Aihara M, Mackey MR, Lindsey JD, Weinreb RN. Regional optic nerve damage in experimental mouse glaucoma. *Invest Ophthalmol Vis Sci*. 2004;45:4352–4358.
32. Zhou Y, Grinchuk O, Tomarev SI. Transgenic mice expressing the Tyr437His mutant of human myocilin protein develop glaucoma. *Invest Ophthalmol Vis Sci*. 2008;49:1932–1939.
33. Jakobs TC, Libby RT, Ben Y, John SWM, Masland RH. Retinal ganglion cell degeneration is topological but not cell type specific in DBA/2J mice. *J Cell Biol*. 2005;171:313–325.
34. Filippopoulos T, Danias J, Chen B, Podos SM, Mittag TW. Topographic and morphologic analyses of retinal ganglion cell loss in old DBA/2NNia mice. *Invest Ophthalmol Vis Sci*. 2006;47:1968–1974.
35. Howell GR, Libby RT, Jakobs TC, et al. Axons of retinal ganglion cells are insulted in the optic nerve early in DBA/2J glaucoma. *J Cell Biol*. 2007;179:1523–1537.
36. Buckingham BP, Inman DM, Lambert W, et al. Progressive ganglion cell degeneration precedes neuronal loss in a mouse model of glaucoma. *J Neurosci*. 2008;28:2735–2744.
37. Soto I, Oglesby E, Buckingham BP, et al. Retinal ganglion cells downregulate gene expression and lose their axons within the optic nerve head in a mouse glaucoma model. *J Neurosci*. 2008;28:548–561.
38. Soto I, Pease ME, Son JL, Shi X, Quigley HA, Marsh-Armstrong N. Retinal ganglion cell loss in a rat ocular hypertension model is sectorial and involves early optic nerve axon loss. *Invest Ophthalmol Vis Sci*. 2011;52:434–441.
39. Minckler DS. The organization of nerve fiber bundles in the primate optic nerve head. *Arch Ophthalmol*. 1980;98:1630–1636.
40. Hoyt WF, Luis O. The primate chiasm: details of visual fiber organization studied by silver impregnation techniques. *Arch Ophthalmol*. 1963;70:69–85.
41. Hoyt WF, Tudor RC. The course of parapapillary temporal retinal axons through the anterior optic nerve: a Nauta degeneration study in the primate. *Arch Ophthalmol*. 1963;69:503–507.
42. Radius RL, Anderson DR. The course of axons through the retina and optic nerve head. *Arch Ophthalmol*. 1979;97:1154–1158.
43. Kimball EC, Pease ME, Steinhart MR, et al. A mouse ocular explant model to study living optic nerve head events after acute and chronic intraocular pressure elevation. *Exp Eye Res*. In press.